

5 Granta-gravel

5.1 Introduction

Previous chapters have been concerned with models that are also discussed in many other books. In this and subsequent chapters we will discuss models that are substantially new, and only a few research workers will be familiar with the notes and papers in which this work was recently first published. The reader who is used to thinking of ‘consolidation’ and ‘shear’ in terms of two dissimilar models may find the new concepts difficult, but the associated mathematical analysis is not hard.

The new concepts are based on those set out in chapter 2. In §2.9 we reviewed the familiar theoretical yield functions of strength of materials: these functions were expressed in algebraic form $F = 0$ and were displayed as yield surfaces in principal stress space in Fig. 2.12. We could compress the work of the next two chapters by writing a general yield function $F=0$ of the same form as eq. (5.27), by drawing the associated yield surface of the form shown in Fig. 5.1, and by directly applying the associated flow rule of §2.10 to the new yield function. But although this could economically generate the algebraic expressions for stress and strain-increments it would probably not convince our readers that the use of the theory of plasticity makes sound mechanical sense for soils. About fifteen years ago it was first suggested¹ that Coulomb’s failure criterion (to which we will come in due course in chapter 8) could serve as a yield function with which one could properly associate a plastic flow: this led to erroneous predictions of high rates of change of volume during shear distortion, and research workers who rejected these predictions tended also to discount the usefulness of the theory of plasticity. Although Drucker, Gibson, and Henkel² subsequently made a correct start in using the associated flow rule, we consider that our arguments make more mechanical sense if we build up our discussion from Drucker’s concept³ of ‘stability’, to which we referred in §2.11.

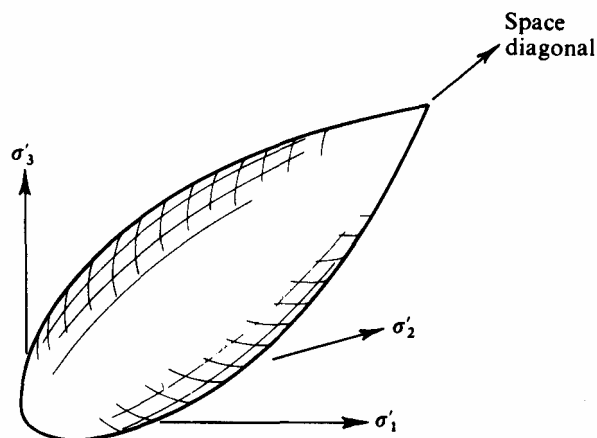


Fig. 5.1 Yield Surface

The concept of a ‘stable material’ needs the setting of a ‘stable system’: we will begin in §5.2 with the description of a system in which a cylindrical specimen of ideal material is under test in axial compression or extension. We will devote the remainder of chapter 5 to development of a conceptual model of an ideal rigid/plastic continuum which has been given the name Granta-gravel. In chapter 6 we will develop a model of an ideal

elastic/plastic continuum called Cam-clay⁴, which supersedes Granta-gravel. (The river which runs past our laboratory is called the Granta in its upper reach and the Cam in the lower reach. The intention is to provide names that are unique and that continually remind our students that these are conceptual materials – not real soil.) Both these models are defined only in the plane in principal stress space containing axial-test data: most data of behaviour of soil-material which we have for comparison are from axial tests, and the Granta-gravel and Cam-clay models exist only to offer a persuasive interpretation of these axial-test data. We hope that by the middle of chapter 6 readers will be satisfied that it is reasonable to compare the mechanical behaviour of real soil-material with the ideal behaviour of an isotropic-hardening model of the theory of plasticity. Then, and not until then, we will formulate a simple critical state model that is an integral part of Granta-gravel, and of Cam-clay, and of other critical state model materials which all flow as a frictional fluid when they are severely distorted. With this critical state model we can clear up the error of the early incorrect application of the associated flow rule to ‘Coulomb’s failure criterion’, and also make a simple and fundamental interpretation of the properties by which engineers currently classify soil.

The Granta-gravel and Cam-clay models only define yield curves in the axial-test plane as shown in Fig 5.2: this curve is the section of the surface of Fig. 5.1 on a diametrical plane that includes the space diagonal and the axis of longitudinal effective stress σ (similar sections of Mises’ and Tresca’s yield surfaces in Fig. 2.12 would show two lines running parallel to the x -axis in the xz -plane). The obvious features of the pear-shaped curve of Fig. 5.2 are the pointed tip on the space diagonal at relatively high pressure, and the flanks parallel to the space diagonal at a lower pressure. A continuing family of yield curves shown faintly in Fig. 5.2 indicates occurrence of stable isotropic hardening. Our first goal in this chapter is to develop a model in the axial-test system that possesses yield curves of this type.

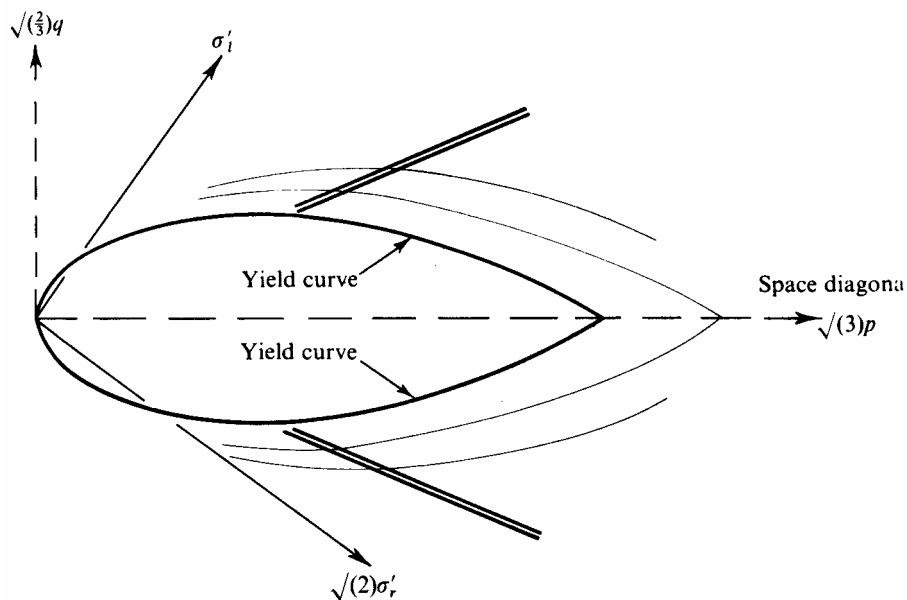


Fig. 5.2 Yield Curves

5.2 A Simple Axial-test System

We shall consider a real axial test in detail in chapter 7: for present purposes a much simplified version of the test system will be described with all dimensions chosen to make the analysis as easy as possible.

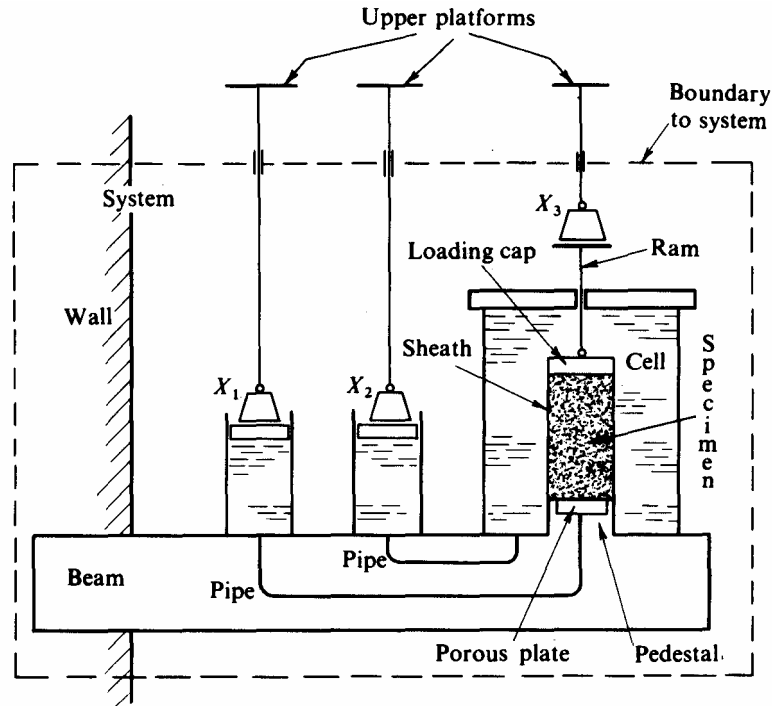


Fig. 5.3 Test System

Let us suppose that we enter a laboratory and find a specimen under test in the apparatus sketched in Fig. 5.3. We first examine the test system and determine the current state of the specimen, which is in *equilibrium* under static loads in a uniform vertical gravitational field. We see that we may probe the equilibrium of the specimen by slowly applying load-increments to some accessible loading platforms. We shall hope to learn sufficient about the mechanical properties of the material to be able to predict its behaviour in any general test.

The specimen forms a right circular cylinder of axial length l , and total volume v , so that its cross-sectional area, $a = v/l$. The volume v is such that the specimen contains unit volume of solids homogeneously mixed with a volume $(v - 1)$ of voids which are saturated with pore-water and free from air.

The specimen stands, with axis vertical, on a pedestal containing a porous plate. The porous plate is connected by a rigid pipe to a cylinder, all full of water and free of air. The pressure in the cylinder is controlled by a piston at approximately the level of the middle of the specimen which is taken as datum. The piston which is of negligible weight and of unit cross-sectional area supports a weight X_1 so that the *pore-pressure* in the specimen is simply $u_w = X_1$.

A stiff impermeable disc forms a loading cap for the specimen. A flexible, impermeable, closely fitting sheath of negligible thickness and strength envelops the specimen and is sealed to the load-cap and to the pedestal. The specimen, with sheath, loading cap, and pedestal, is immersed in water in a transparent cell. The cell is connected by a rigid pipe to a cylinder where a known weight X_2 rests on a piston of negligible weight and unit cross-sectional area. The cell, pipe, and cylinder are full of water and free from air, so that the cell pressure is simply $\sigma_r = X_2$ which is related to the same datum as the pore-pressure. The cell pressure is the principal *radial total stress* acting on the cylindrical specimen.

A thin stiff ram of negligible weight slides freely through a gland in the top of the cell in a vertical line coincident with the axis of the specimen. A weight X_3 rests on this

ram and causes a vertical force to act on the loading cap and a resulting axial pressure to act through the length of the specimen. In addition, the cell pressure σ_r acts on the loading cap and, together with the effect of the ram force X_3 , gives rise to the principal *axial total stress* σ_l experienced by the specimen, so that

$$X_3 = a(\sigma_l - \sigma_r).$$

Hence, three stress quantities u_w , σ_r and $(\sigma_l - \sigma_r)$, and two dimensional quantities v , and l , describe the state of the specimen as it stands in equilibrium in the test system.

5.3 Probing

The *test system* of Fig. 5.3 is encased by an imaginary boundary which is penetrated by three stiff, light rods of negligible weight shown attached to the main loads X_1 , X_2 , and X_3 . These rods can slide freely in a vertical direction through glands in the boundary casing, and they carry upper platforms to which small load-increments can be applied or removed. The displacement of any load-increment is identical to that of its associated load within the system, being observed as the movement of the upper platform.

We imagine ourselves to be an *external agency* standing in front of this test system in which a specimen is in equilibrium under relatively heavy loads: we test its stability by gingerly prodding and poking the system to see how it reacts. We do this by conducting a *probing* operation which is defined to be the slow application and slow removal of an infinitesimally small load-increment. The *load-increment* itself consists of a set of loads $\dot{X}_1, \dot{X}_2, \dot{X}_3$ (any of which may be zero or negative) applied simultaneously to the three upper platforms, see Fig. 5.4.

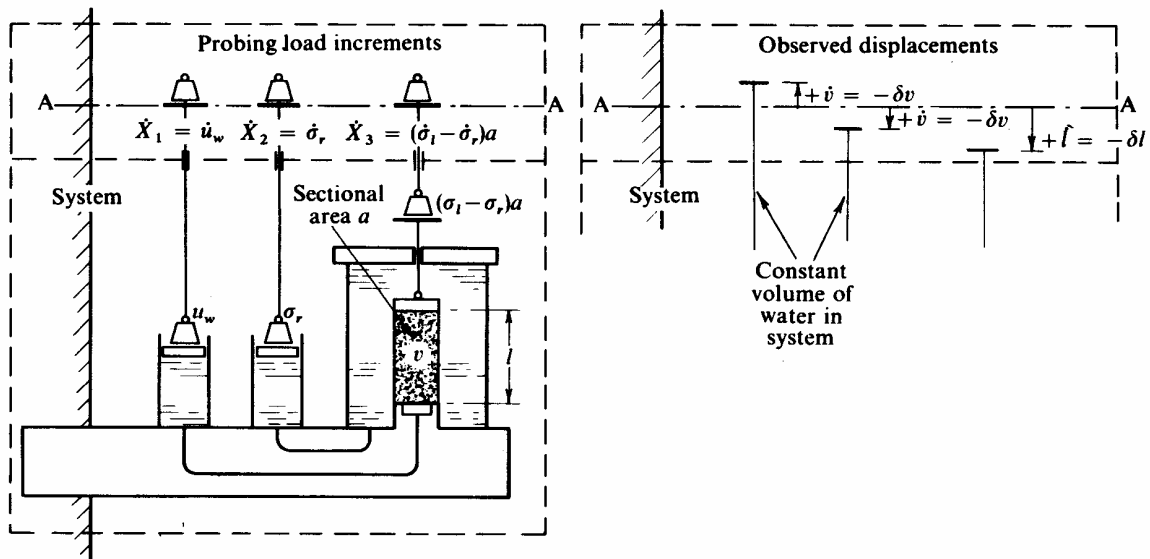


Fig. 5.4 Probing Load-increments

Each application and removal of load-increment will need to be so slow that it is at all times fully resisted by the effective stresses in the specimen, and at all times excess pore-pressures in the specimen are negligible. If increments were suddenly placed on the platforms work would be done making the pore-water flow quickly through the pores in the specimen.

We use the term *effectively stressed* to describe a state in which there are no excess pore-pressures within the specimen, i.e., load and load-increment are both acting with full

effect on the specimen. In Fig. 5.5(a) **OP** represents the slow application of a single load-increment \dot{X} fully resisted by the slow compression of an effectively stressed specimen, and **PO** represents the slow removal of the load-increment \dot{X} exactly matched by the slow swelling of the effectively stressed specimen. It is clear that, in the cycle **OPO**, by stage P the external agency has slowly transferred into the system a small quantity of work of magnitude $(1/2)\dot{X}\delta$, and by the end **O** of the cycle this work has been recovered by the external agency without loss.

In contrast in Fig. 5.5(b) **OQ** represents a sudden application of a load-increment \dot{X} at first resisted by excess pore-pressures and only later coming to stress effectively the specimen at R. During the stage **QR** a quantity of work of magnitude $\dot{X}\delta$ is transferred into the system, of which a half (represented by area OQR) has been dissipated within the system in making pore-water flow quickly and the other half (area ORS) remains in store in the effectively stressed specimen. Stage **RS** represents the sudden removal of the whole small load-increment \dot{X} from the loading platform when it is at its low level. Negative pore-pressure gradients are generated which quickly suck water back into the specimen, and by the end of the cycle at O the work which was temporarily stored in the specimen has all been dissipated. At the end of the loading cycle the small load increment is removed at the lower level, and the external agency has transferred *into* the system the quantity of work $\dot{X}\delta$ indicated by the shaded area **OQRS** in Fig.5.5(b), although the effectively stressed material structure of the specimen has behaved in a reversible manner. In a study of work stored and dissipated in effectively stressed specimens it is therefore essential to displace the loading platforms slowly.

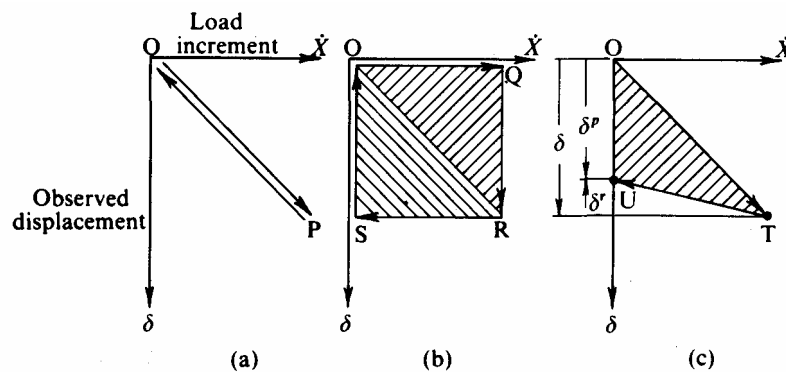


Fig. 5.5 Work Done during Probing Cycle

For the most general case of probing we must consider the situation shown in Fig. 5.5(c) in which the loading platform does not return to its original position at the end of the cycle of operations, and the specimen which has been effectively stressed throughout has suffered some permanent deformation. The total displacement δ observed after application of the load-increment has to be separated into a component δ^r which is *recovered* when the load-increment is removed and a *plastic* component δ^p which is not.

Because we shall be concerned with quantities of *work* transferred into and out of the test system, and not merely with displacements, we must take careful account of signs and treat the displacements as *vector* quantities. Since we can only discover the plastic component as a result of applying and then removing a load-increment, we must write it as the resultant of initial, total, and subsequently recovered displacements

$$\delta^p = \delta + \delta^r.$$

When plastic components of displacement occur we say that the specimen *yields*. As we have already seen in §2.9 and §2.10 we are particularly interested in the states in which the specimen will yield, and in the nature of the infinitesimal but irrecoverable displacements that occur when the specimen yields.

5.4 Stability and Instability

Underlying the whole previous section is the tacit assumption that it is within our power to make the displacement diminishingly small: that if we do virtually nothing to disturb the system then virtually nothing will happen. We can well recall counter-examples of systems which failed when they were barely touched, and if we really were faced with this axial-test system in equilibrium under static loads we would be fearful of failure: we would not touch the system without attaching some buffer that could absorb as internal or potential or inertial energy any power that the system might begin to emit.

If the disturbance is small then, whatever the specimen may be, we can calculate the net quantity of work transferred across the boundary *from* the external agency *to* the test system, as

$$\sum \frac{1}{2} \dot{X}_i \delta_i^p.$$

For example, with the single probing increment illustrated in Fig. 5.5(c) this net quantity of work equals the shaded area Δ AOTU. If the specimen is *rigid*, then $\delta_i^p \equiv 0 \equiv \delta_i^r$, and the probe has no effect. If the specimen is *elastic* (used in the sense outlined in chapter 2) then $\delta_i^p \equiv 0$, all displacement is recoverable and there is no net transfer of work at the completion of the probing cycle. If the specimen is *plastic* (also used in the sense outlined in chapter 2) then some net quantity of work will be transferred to the system. In each of these three cases the system satisfies a *stability criterion* which we will write as

$$\sum \dot{X}_i \delta_i^p \geq 0, \quad (5.1)$$

and we will describe these specimens as being made of *stable material*.

In a recent discussion Drucker⁵ writes of

‘the term *stable material*, which is a specialization of the rather ill-defined term *stable system*.

A stable system is, qualitatively, one whose configuration is determined by the history of loading in the sense that small perturbations produce a small change in response and that no spontaneous change in configuration will occur. Quantitative definition of the terms *stable*, *small*, *perturbation*, and *response* are not clear cut when irreversible processes are considered, because a dissipative system does not return in general to its original equilibrium configuration when a disturbance is removed. Different degrees of stability may exist.’

Our choice of the stability* criterion (5.1) enables us to distinguish two classes of response to probing of our system:

I *Stability*, when a cycle of probing of the system produces a response satisfying the criterion (5.1), and

II *Instability*, when a cycle of probing of the system produces a response violating the criterion (5.1).

* This word will only be used in one sense in this text, and will always refer to material stability as discussed in §2.11 and here in §5.4. It will *not* be used to describe limiting-stress calculations that relate to failure of soil masses and are sometimes called ‘slope-stability’ or ‘stability-of-foundation’ calculations. These limiting-stress calculations will be met later in chapter 9.

The role of an external attachment in moderating the consequence of instability can be illustrated in Fig. 5.6. The axial-test system in that figure has attached to it an arrangement in which instability of the specimen permits the transfer of work out of the system: Fig. 5.6(a) shows a pulley fixed over the relatively large ram load with a relatively small *negative* load-increment ($\dot{X}_3 < 0$) applied by attaching a small weight to the chord round the pulley. At the same time a small *positive* load-increment ($\dot{X}_1 > 0$) is applied to the pore pressure platform, and we suppose that, for some reason which need not be specified here, the change in pore-pressure happens to result, as shown in Fig. 5.6(b), in unstable compressive failure of the specimen at constant volume. The large load on the ram will fall as the specimen fails, and in doing so will raise the small load-increment. The external probing agency has thus provoked a release of usable *work from the system*. In general, the loading masses within the system would take up energy in acceleration, and we would observe a sudden uncontrollable displacement of the loading platforms which we would take to indicate *failure* in the system.

The study of systems at failure is problematical. The load-increment sometimes brings parts of a test system into an unstable configuration where failure occurs, even though the specimen itself is in a state which would not appear unstable in another test in another system. In contrast, the study of stable test systems leads in a straightforward manner, as is shown below, to development of stress – strain relationships for the specimen under test. Once these relationships are known they may be used to solve problems of failure.

It is essential to distinguish *stable* states from the wider class of states of static *equilibrium* in general. A simple calculation of virtual work within the system boundary based on some virtual displacement of parts of a system, would be sufficient to check that the system is in static equilibrium, but additional calculations are needed to guarantee stability. Engineers generally must design systems not only to perform a stated function but also to continue to perform properly under changing conditions. A small change of external conditions must only cause a small error in predicted performance of a well engineered system. For each state of the system, we check carefully to ensure that there is no accessible alternative state into which probing by an external agency can bring the system and cause a net emission of power in a probing cycle.

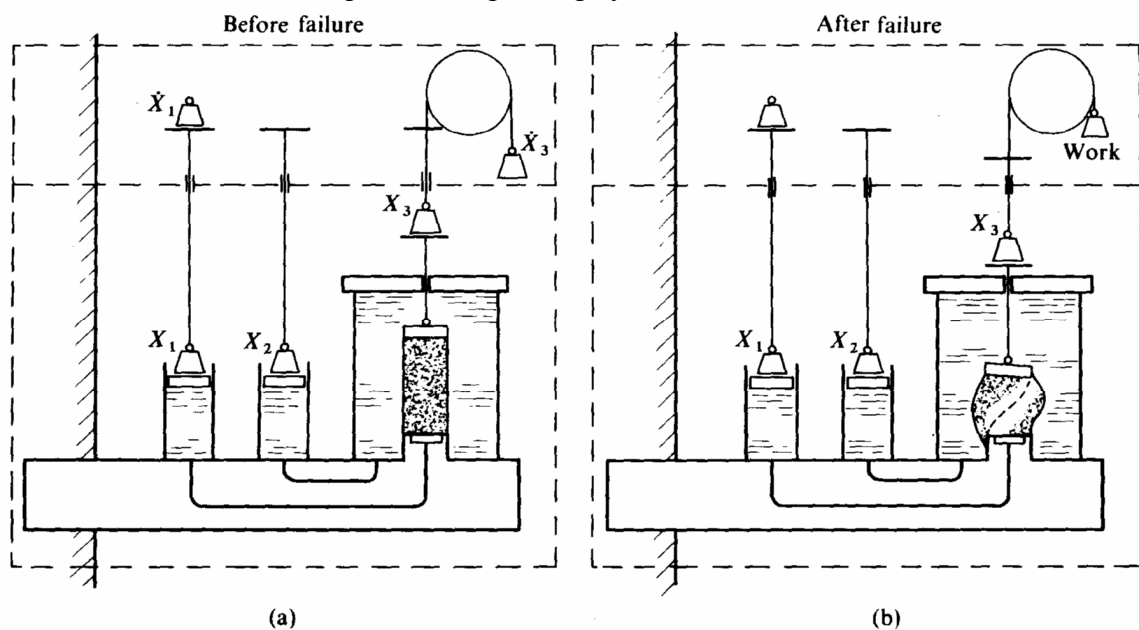


Fig. 5.6 Unstable Yielding

In the following sections we begin by considering the stressed state of the specimen and the increments of stress and strain. Then come calculations about power, and the use of power in the system. This leads to certain interesting calculations, but in §5.10 we will return to this stability criterion and make use of it to explain why it is that in some states some load-increments make the specimens yield and others do not. The stability criterion is essential to this chapter, but before developing it in detail we must select appropriate parameters.

5.5 Stress, Stress-increment, and Strain-increment

Let the state of effective stress experienced by the specimen be separated into *spherical* and *deviatoric* components, in the same manner that proved helpful to an understanding of the mechanical behaviour of elastic material in §2.6 and §2.7. The *total* stresses acting on the specimen u_w , σ_r , and σ_l can be used to define parameters somewhat similar to eq. (2.4):

effective spherical pressure

$$p = \frac{\sigma_l + 2\sigma_r}{3} - u_w > 0 \quad (5.2)$$

and axial-deviator stress

$$q = \sigma_l - \sigma_r. \quad (5.3)$$

In Fig. 5.2 the space diagonal axis has units of $\sqrt{(3)}p$ and the perpendicular axis has units $\sqrt{(2/3)}q$; an alternative and simpler representation of the state of stress of the axial-test specimen is now given in Fig. 5.7 where axes p and q are used directly without the multiplying factors $\sqrt{(3)}$ and $\sqrt{(2/3)}q$.

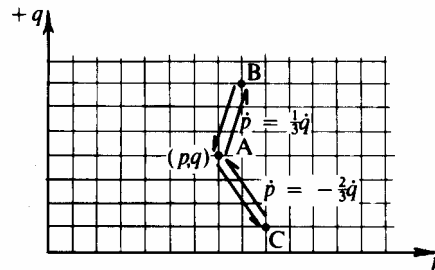


Fig. 5.7 Stress Paths Applied by Probes

In a corresponding manner, parameters of stress-increment can be calculated and used to describe any load-increment, namely:

effective spherical pressure increment

$$\dot{p} = \frac{\dot{\sigma}_l + 2\dot{\sigma}_r}{3} - \dot{u}_w \quad (5.4)$$

and axial-deviator stress-increment

$$\dot{q} = \dot{\sigma}_l - \dot{\sigma}_r. \quad (5.5)$$

The parameters (\dot{p}, \dot{q}) define a vector in the (p, q) plane, and Fig. 5.7 illustrates two examples. In each example the specimen drains into the pore-pressure cylinder with no pore-pressure load-increment, $\dot{u}_w \equiv 0$. One example, AB, (equivalent to a conventional drained compression test) involves load-increment only on the ram platform and not on the cell pressure platform so that

$$\dot{\sigma}_r = 0, \quad \dot{\sigma}_l = \frac{\dot{X}_3}{a} > 0.$$

In this example, eqs. (5.4) and (5.5) give

$$\dot{p} = \frac{1}{3} \dot{\sigma}_l \quad \dot{q} = \dot{\sigma}_l \quad \frac{\dot{p}}{\dot{q}} = \frac{1}{3}$$

so that the load-increment brings the specimen into a state of stress represented on the (p, q) plane by some point B on the line through A of slope 3 given by $\dot{p} = \frac{1}{3} \dot{q}$. The probing cycle would be completed by removal of the load-increment and return of the specimen to the original stress state at A (though not necessarily to the original lengths and volumes).

The second example, AC (equivalent to a drained extension test), involves load-increment on the cell pressure platform and an equal but opposite negative stress-increment on the ram platform, so that $\dot{\sigma}_l = 0, \dot{\sigma}_r = \dot{X}_2 = -\dot{X}_3 / a > 0$. In that case eqs. (5.4) and (5.5) give

$$\dot{p} = \frac{1}{3} \dot{\sigma}_r \quad \dot{q} = -\dot{\sigma}_r \quad \frac{\dot{p}}{\dot{q}} = -\frac{2}{3}$$

so that the load-increment brings the specimen into a state represented in the (p, q) plane by some point C on a line through A of slope $-\frac{3}{2}$ given by $\dot{p} = -\frac{2}{3} \dot{q}$. As before, completion of the probing cycle requires removal of load increments, and a return to a state represented by point A.

The choice of strain-increment parameters to correspond to (p, \dot{p}) and (q, \dot{q}) requires care. It is essential that when the corresponding stress and strain-increments are multiplied together they correctly give the incremental work per unit volume performed by stresses on the specimen. This essential check will be carried out in the next section, §5.6. But in introducing the strain-increment parameters an appeal to intuition is helpful. Clearly, change in specimen volume can be chosen to correspond with effective spherical pressure and pressure increment. The choice of a strain parameter to correspond with axial-deviator stress and stress-increment is not so obvious. The ram displacement l does not correspond simply to axial-deviator stress; indeed, if an elastic specimen is subjected to effective spherical pressure increment without any axial-deviator stress there will be a longitudinal strain of one third of the volumetric strain. This suggests the possibility of defining a parameter⁶ called axial-distortion increment

$$+ \dot{\epsilon} = \frac{\dot{l}}{l} - \frac{1}{3} \frac{\dot{v}}{v} \quad (5.6)$$

to correspond to axial-deviator stress. The correctness of this choice will be shown in §5.6.

Care must be taken with signs of these parameters. Since stress is defined to be positive in compression, it is necessary to define length *reduction* and radius *reduction* as *positive* strain-increments, $\dot{\epsilon}_l$ and $\dot{\epsilon}_r$, respectively. Then defining longitudinal strain-increment as

$$\left. \begin{aligned} \dot{\epsilon}_l &= \frac{\dot{l}}{l} = -\frac{\delta l}{l} \\ \text{and radial strain - increment as} \\ \dot{\epsilon}_r &= \frac{\dot{r}}{r} = -\frac{\delta r}{r} \end{aligned} \right\} \quad (5.7)$$

we have volumetric strain-increment,

$$\frac{\dot{v}}{v} = -\frac{\delta v}{v} = \dot{\epsilon}_l + 2\dot{\epsilon}_r \quad (5.8)$$

and eq. (5.6) can be re-written

$$\dot{\epsilon} = \frac{2}{3} (\dot{\epsilon}_l - \dot{\epsilon}_r). \quad (5.9)$$

It will be appropriate to distinguish between deformations called
length reduction when $\dot{\epsilon} > 0$

and *radius reduction* when $\dot{\epsilon} < 0$.

A little conceptual difficulty may be met later because volumetric strain-increment has been defined in eq. (5.8) to be positive when the volume v is being reduced.

It should be noted that for this choice of parameters to be meaningful principal axes of stress, stress-increment, and strain-increment must coincide.

5.6 Power

The rate (with respect to strain*) of working of the main loading *within the system* on the specimen during the displacements provoked by the external agency will be called the *loading power* of the system. It can be simply calculated from the observed displacements of Fig. 5.4 to be

$$\dot{E} = -u_w \dot{v} + \sigma_r \dot{v} + (\sigma_l - \sigma_r) a \dot{l}. \quad (5.10)$$

The upward displacement of the pore-pressure piston is equal and opposite to the downward displacement of the cell-pressure piston, and so the loading power depends only on the effective stresses

$$\sigma'_r = \sigma_r - u_w \quad \sigma'_l = \sigma_l - u_w$$

and eq. (5.10) can be re-written

$$\dot{E} = \sigma'_r \dot{v} + (\sigma'_l - \sigma'_r) a \dot{l}.$$

Introducing eqs. (5.7) and (5.8), the loading power per unit volume of specimen becomes

$$\begin{aligned} \frac{\dot{E}}{v} &= \sigma'_r \frac{\dot{v}}{v} + (\sigma'_l - \sigma'_r) \frac{\dot{l}}{l} \\ &= \sigma'_r (\dot{\epsilon}_l + 2\dot{\epsilon}_r) + (\sigma'_l - \sigma'_r) \dot{\epsilon}_l \\ &= \sigma'_l \dot{\epsilon}_l + 2\sigma'_r \dot{\epsilon}_r, \end{aligned} \quad (5.1)$$

in which form the rate of working of effective stresses moving at their respective strain rates is directly evident.

But from eqs. (5.2), (5.3), (5.8), and (5.9) we obtain

$$\left. \begin{aligned} p \frac{\dot{v}}{v} &= \left(\frac{\sigma'_l + 2\sigma'_r}{3} \right) (\dot{\epsilon}_l + 2\dot{\epsilon}_r) = \frac{\sigma'_l \dot{\epsilon}_l}{3} + \frac{4\sigma'_r \dot{\epsilon}_r}{3} + \frac{2\sigma'_r \dot{\epsilon}_l}{3} + \frac{2\sigma'_l \dot{\epsilon}_r}{3} \\ \text{and} \\ q \dot{\epsilon} &= \frac{2}{3} (\sigma'_l - \sigma'_r) (\dot{\epsilon}_l - \dot{\epsilon}_r) = \frac{2\sigma'_l \dot{\epsilon}_l}{3} + \frac{2\sigma'_r \dot{\epsilon}_r}{3} - \frac{2\sigma'_r \dot{\epsilon}_l}{3} - \frac{2\sigma'_l \dot{\epsilon}_r}{3} \end{aligned} \right\}$$

which when added give

$$p \frac{\dot{v}}{v} + q \dot{\epsilon} = \sigma'_l \dot{\epsilon}_l + 2\sigma'_r \dot{\epsilon}_r. \quad (5.12)$$

This confirms the correctness of the choice of strain-increment parameters, because comparison of eqs. (5.11) and (5.12) shows that

$$\frac{p \dot{v}}{v} + q \dot{\epsilon} = \frac{\dot{E}}{v} \quad (5.13)$$

which is clearly necessary.

* Equations of the theory of plasticity are independent of time.⁷

At this juncture we must recall the mechanical working of the system and the external agency, see Fig. 5.4. The loads within the casing of the test system are relatively heavy and they may well have brought the specimen to the point of yielding. The object of the tests is to learn how this loaded specimen will adjust itself when it is gently probed. During the small displacements that are provoked by the external agency the heavy loads moving within the system generate power \dot{E} which the specimen must either store or dissipate: in the following section §5.7 we will define the nature of the Granta-gravel material by stating the manner in which it disposes of this loading power. All this is taking place *within* the system. In addition, there is the small power input \dot{P} by which the external agency is controlling, and at the same time provoking, the displacements of the system, given by

$$\frac{\dot{P}}{v} = \frac{1}{2} \left(\dot{p} \frac{\dot{v}}{v} + q \dot{\epsilon} \right).$$

This power is transmitted across the casing or boundary of the system during application of the load-increment, but it is altogether smaller than the power of the heavy loads that are causing the specimen to deform. We think of \dot{P} as a small input signal that controls the powerful heavy loads within the system.

During application of the load-increment the loading power per unit volume transferred from the heavy loads to the specimen is, from eq. (5.13),

$$\frac{\dot{E}}{v} = \left(\frac{p \dot{v}}{v} + q \dot{\epsilon} \right).$$

During subsequent unloading the recoverable power per unit volume returned by the specimen to the heavy loads within the system is

$$+ \frac{\dot{U}}{v} = - \left(\frac{p \dot{v}^r}{v} + q \dot{\epsilon}^r \right). \quad (5.14)$$

The remainder of the loading power which is not transferred back and has been dissipated within the specimen is

$$\frac{\dot{W}}{v} = \frac{\dot{E}}{v} - \frac{\dot{U}}{v} = - \left(\frac{p \dot{v}^p}{v} + q \dot{\epsilon}^p \right). \quad (5.15)$$

Of course transfers from heavy loads to specimen and back again do not involve any transfer across the casing that surrounds the system. However, there may be some *net* work transferred by the external probing agency across the boundary to the system in the complete probing cycle, which is the small quantity

$$\frac{1}{2} \left(\dot{p} \frac{\dot{v}^p}{v} + q \dot{\epsilon}^p \right) = \sum \frac{1}{2} \dot{X}_i \delta_i^p$$

corresponding to the shaded area in Fig. 5.5(c). We have already discussed the importance of this in §5.4 and seen that our criterion of stability (5.1) requires

$$\dot{p} \frac{\dot{v}^p}{v} + q \dot{\epsilon}^p \geq 0. \quad (5.16)$$

5.7 Power in Granta-gravel

To specify the mechanical behaviour of a material it is necessary to prescribe the nature of the four terms on the right of eqs. (5.14) and (5.15). For example, if a gas were tested only the first term of the first equation $\frac{p \dot{v}^r}{v}$ would be significant and all the other terms would be negligible. Again, if a perfectly elastic material were tested \dot{v}^p and

$\dot{\varepsilon}^p$ would be zero, and \dot{v}^r and $\dot{\varepsilon}^r$ might be prescribed functions of p, \dot{p} and q, \dot{q} . In formulating an artificial material we are free to choose what ingredients we like for the recipe provided by these two equations. We require Granta-gravel to be an *ideal rigid/plastic material* and so we shall take as our first and major simplification the requirement that it *never displays any recoverable strains*, i.e.,

$$\dot{v}^r \equiv \dot{\varepsilon}^r \equiv 0. \quad (5.17)$$

This means that the application of a probing load-increment either meets with a rigid response, or causes yield, but that the subsequent removal of the load-increment has no effect at all. There can be no recoverable power \dot{U} and all loading power \dot{E} is dissipated within the specimen as \dot{W} .

We need to specify how this work \dot{W} is dissipated, and as Granta-gravel is intended to be as simple a model as possible of a frictional granular material we shall assume that

$$\frac{\dot{W}}{v} = Mp|\dot{\varepsilon}| > 0. \quad (5.18)$$

In this equation M (capital μ) is a simple frictional constant so that \dot{W} is linearly dependent on $p > 0$. The modulus sign is required for $\dot{\varepsilon}$ because frictional work is always dissipated and \dot{W} must always be positive. This property of Granta-gravel is a sort of ‘friction’ in the sense loosely defined in §1.8.

Combining these assumptions and re-writing eqs. (5.14), (5.15), and (5.16) we have specified for Granta-gravel

$$\begin{aligned} \dot{v}^r \equiv \dot{\varepsilon}^r \equiv 0 \quad \dot{v} \equiv \dot{v}^p \quad \dot{\varepsilon} \equiv \dot{\varepsilon}^p \quad \dot{U} \equiv 0 \\ \frac{p\dot{v}}{v} + q\dot{\varepsilon} = \frac{\dot{W}}{v} = Mp|\dot{\varepsilon}| \end{aligned} \quad (5.19)$$

and the stability criterion becomes

$$\frac{\dot{p}\dot{v}}{v} + \dot{q}\dot{\varepsilon} \geq 0. \quad (5.20)$$

5.8 Responses to Probes which cause Yield

If we have a specimen of Granta-gravel of specific volume v_1 under test, in equilibrium at the stressed state (p_1, q_1) , and we apply a series of different probes (\dot{p}, \dot{q}) , we can now use eq. (5.19) to predict responses of the system. Generally, the specimen remains *rigid* but there may be certain probes which cause it to *yield*, and when yielding occurs the power equation (5.19) tells us what ratio of (permanent) increments of strain the specimen will experience.

For the case of length reduction, $\dot{\varepsilon} > 0$, we have

$$\frac{\dot{v}}{v_1\dot{\varepsilon}} = +M - \frac{q_1}{p_1} \quad (5.21a)$$

and for radius reduction, $\dot{\varepsilon} < 0$,

$$\frac{\dot{v}}{v_1\dot{\varepsilon}} = -M - \frac{q_1}{p_1}. \quad (5.21b)$$

These equations provide relationships between stress ratio $\eta_1 = (q_1/p_1)$ and strain-increment ratio $\dot{v}/v_1\dot{\varepsilon}$, and reveal the importance of the constant M . We will describe specimens which yield when $|q_1| < Mp_1$ as being *weak at yield*, and those which yield when $|q_1| > Mp_1$ as

being *strong at yield*, and those which yield when $|q_1| = Mp_1$ as being in a *critical state* at yield.

At this stage, in order to develop the argument economically, we shall confine our attention to specimens that are experiencing a *positive* deviator stress, $q_1 > 0$, and subject to reduction of length $\dot{\epsilon} \geq 0$. This is equivalent to conducting conventional axial compression tests only, but we shall see later that this restriction does not cause loss of generality, as similar results can be obtained for extension tests where $q_1 < 0$ and $\dot{\epsilon} \leq 0$.

5.9 Critical States

Although we are taking $q_1 > 0$ and $\dot{\epsilon} \geq 0$ we still have three distinct classes of specimen to consider:

- $q_1 < Mp_1$ for which eq. (5.21a) shows that $\dot{v} = -\delta v > 0$ so that all specimens weak at yield must be *compacting*,
- $q_1 > Mp_1$ for which we must have $\dot{v} = -\delta v < 0$ so that all specimens strong at yield must be *dilating*,
- $q_1 = Mp_1$ for which $\dot{v} = 0$ so that specimens yielding in what we call ‘critical states’ remain at constant volume, $\dot{\epsilon}$ is indeterminate, and in these states yield can continue to occur without change in q_1 , p_1 , or v_1 . The material behaves as a *frictional fluid* rather than a yielding *solid*; it is as though the material had melted under stress.

The behaviour of each of these three classes (a), (b), and (c) is indicated in Fig. 5.8 from which it is clear that when the states of

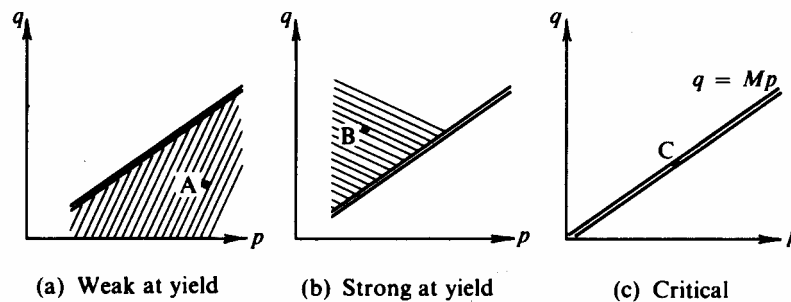


Fig. 5.8 Condition of Specimens at Yield in Relation to Line of Critical States

specimens are represented by the parameters (p, v) in Fig. 5.9 a distinct curve separates an area in which yielding specimens compact, from one in which they dilate. In addition, any point such as C appropriate to a specimen yielding in a critical state with $q_1 = Mp_1, v = v_1$ must lie on this curve.

Experimental evidence⁸⁻¹¹ supports the assumption that for specimens of Granta-gravel in tests with length reduction there exists a unique curve of *critical states* in (p, v, q) space. This curve, which will always be shown in diagrams as a double line, is given by the pair of equations

$$q = Mp \quad (5.22)$$

defining the straight line projection in Figs. 5.8(a), (b), and (c),

$$\text{and} \quad v = \Gamma - \lambda \ln p \quad (5.23)$$

defining the projected *critical curve* of Fig. 5.9. (We shall expect a mirror image of this critical state curve on the negative side of the $q = 0$ plane for tests with radius reduction.)

It is experimentally difficult to keep a specimen under control as it approaches the critical state and tends towards frictional fluid behaviour. Axial-test specimens have closely defined right-cylindrical shape at the start of a test, but we can clearly see them lose shape and we must expect that the test system will become unstable and exhibit 'failure' before average conditions in the specimen correspond closely to critical conditions. However, leaving to one side at present the difficulties of the specific system of Figs. 5.3, 5.4, 5.6, it is necessary to idealize and assume that specimens of Granta-gravel can reach a critical state.

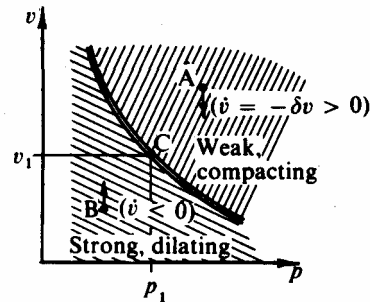


Fig. 5.9 Line of Critical States for Length Reduction

5.10 Yielding of Granta-gravel

From our outline of theory of plasticity in chapter 2 we expect the permissible stressed states of a particular specimen of Granta-gravel to be bounded by a convex closed *yield curve* in the axial-test plane or the (p, q) plane of Fig. 5.10. We expect that under changes of states of stress represented by paths within the boundary, such as from L to K, the specimen of Granta-gravel will remain rigid with no displacements and with its specific volume unchanged at v_1 .

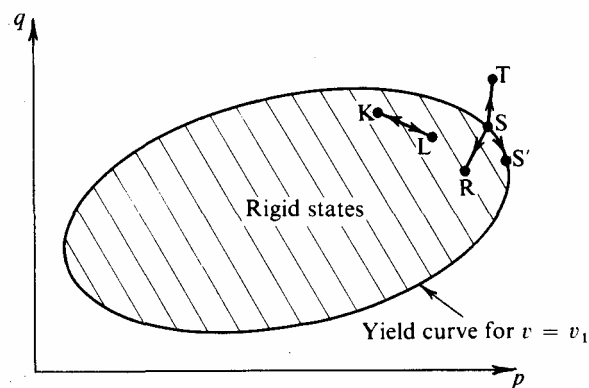


Fig. 5.10 Closed Convex Yield Curve

Let us examine in detail the behaviour of a specimen under the state of stress given by S, which is on the yield curve with coordinates (p_s, q_s) . We can apply a variety of infinitesimal probes (\dot{p}, \dot{q}) , as a result of which the specimen either remains rigid or yields with permanent deformations satisfying eq. (5.19). The inequality (5.20) tells us whether such yielding is stable or unstable. Combining these and eliminating \dot{v} we obtain the inequality

$$\dot{p}(Mp_s|\dot{\epsilon}| - q_s\dot{\epsilon}) + p_s\dot{q}\dot{\epsilon} \geq 0$$

and since we have previously specified $\dot{\epsilon} \geq 0$ we have the requirement for *stable yielding*

$$\left(M - \frac{q_s}{p_s} \right) \dot{p} + \dot{q} > 0, \quad \dot{\epsilon} > 0. \tag{5.24}$$

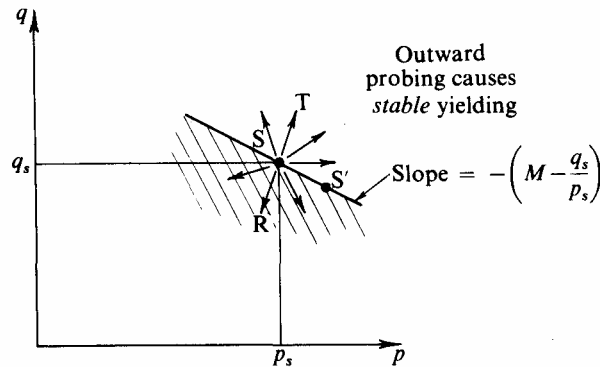


Fig. 5.11 Probing Vectors at Point on Yield Curve

Considering in Fig. 5.11 all possible probing vectors at the point S, we can now distinguish between those such as ST which are directed *outwards* from a line through S of slope

$$\frac{dq}{dp} = \frac{\dot{q}}{\dot{p}} = - \left(M - \frac{q_s}{p_s} \right) \tag{5.25}$$

those such as SR which are directed *inwards* from the line, and those such as SS' which are directed *along* the line. Under the first of these probings yielding would satisfy the stability criterion and inequality (5.24): under the second of these probings rigidity must be postulated so that $\dot{\epsilon}$ is zero if the stability criterion is to be satisfied: under the third of these probings the specimen experiences a *neutral* change of state in which it moves into an adjacent state of limiting rigidity, still on the point of yielding.

In this manner we can link the stability criterion with the theory of plasticity, as also set out in chapter 2. We can integrate eq. (5.25) to give

$$\frac{q}{Mp} = \ln p = \text{const.} \tag{5.26}$$

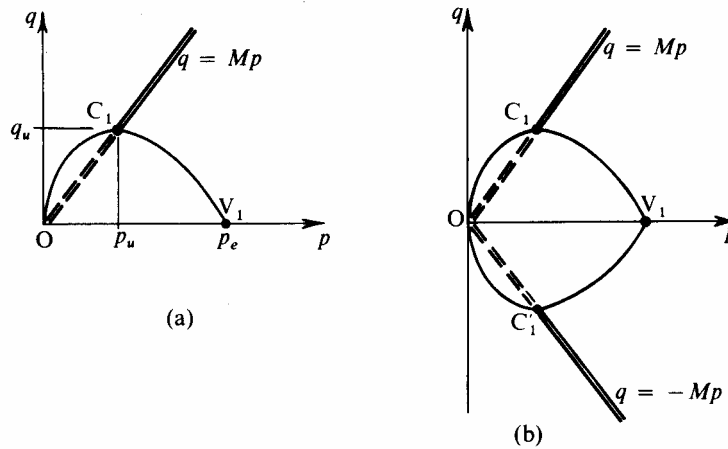


Fig. 5.12 Yield Curve for Specimens of Granta-gravel of Volume v_1

We can evaluate the constant of integration as we know that the yield curve must pass through the critical state C_1 appropriate to this specimen of specific volume v_1 . Let this be denoted by $(p_u, q_u = Mp_u)$ so that the yield curve becomes

$$\frac{q}{Mp} + \ln\left(\frac{p}{p_u}\right) = 1 \quad (q > 0). \quad (5.27)$$

Our argument has been confined so far to loads with $q > 0$ so the yield curve given by eq. (5.27) is confined to the positive quadrant as shown in Fig. 5.12(a). If the argument of this and the last section (5.9) is now repeated for specimens subject to negative deviator stress $q < 0$ and reduction of radius $\dot{\epsilon} \leq 0$ (equivalent to a conventional extension test) we shall get exactly similar expressions but with appropriate changes of sign throughout, and derive a yield curve which is the mirror image of that above, i.e.,

$$-\frac{q}{Mp} + \ln\left(\frac{p}{p_u}\right) = 1 \quad (q > 0). \quad (5.28)$$

Putting the two together we have established a symmetrical closed convex curve, Fig. 5.12(b). The main features of this curve are that it passes through the origin (with the q -axis as tangent), has zero gradient at the critical states C_1 and C'_1 , and has a vertex at V_1 where the gradients are $\pm M$. In particular, the pressure at the vertex denoted by P_e is such that $\ln(p_e / p_u) = 1$, i.e.,

$$p_e = 2.718p_u. \quad (5.29)$$

It must be remembered that the yield curve *only* applies to specimens of the particular specific volume $v=v_1$ that we have considered, and that it is a boundary containing *all* permissible equilibrium states of stress for this set of specimens. Mathematically, in eqs. (5.27) and (5.28) it is the parameter p_u which is a unique function of v_1 . In the next section we will consider the family of yield curves that apply to sets of specimens of other specific volumes.

5.11 Family of Yield Curves

In the last section we established the yield curve of Fig. 5.12(b) for specimens of specific volume v_1 . If instead we have a specimen of different specific volume v_2 , the appropriate critical states C_2 and C'_2 will have moved to a different position (p_u, v_u) on the critical curve of Figs. 5.9 and 5.13 dictated by

$$v = \Gamma - \lambda \ln p. \quad (5.23 \text{ bis})$$

We shall have a second yield curve of identical shape but of different size, with the position of C (and C') acting as a scaling factor. Both of these curves clearly belong to a nest or family of yield curves.

This family of curves generates a closed surface in the three-dimensional space (p, v, q) which must contain all permissible states of specimens; it will not be possible for a specimen to be in stable equilibrium in a state represented by a point outside this surface. Hence it is called⁹ the *stable-state boundary surface* and is represented by the single equation

$$|q| = Mp \left(1 + \frac{\Gamma - v}{\lambda} - \ln p \right) \quad (5.30)$$

obtained from eqs. (5.23) and the pair (5.27) and (5.28). A view of the surface is best seen in the direction of the arrow of Fig. 5.13; and the upper half is shown thus in Fig. 5.14.

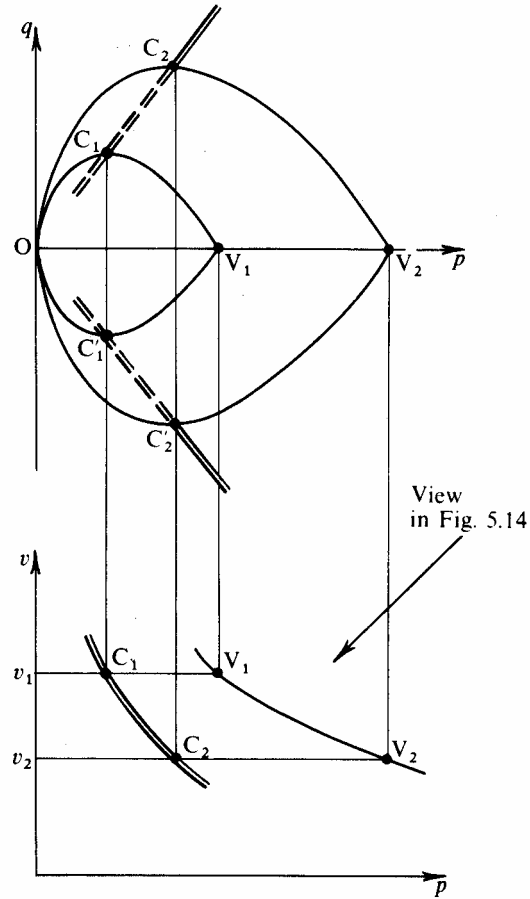


Fig. 5.13 Separate Yield Curves for Specimens of Different Volumes

If we consider a set of specimens all at the same ratio $\eta = q/p > 0$ at yield, we see from substitution in eq. (5.30) that their states must lie on the line

$$v + \lambda \ln p = \lambda \left(1 - \frac{\eta}{M} \right) + \Gamma = \text{const.} \tag{5.31}$$

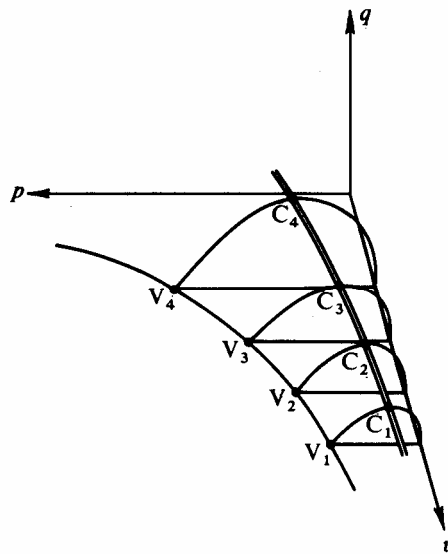


Fig. 5.14 Upper Half of State Boundary Surface

This is illustrated in Fig. 5.15; where each curve, $v + \lambda \ln p = \text{constant}$, corresponds to one value of η and vice versa. The critical curve $C_1C_2C_3$ and the curve joining the vertices $V_1V_2V_3$ are seen to be special members of this set. If the lower diagram, Fig. 5.15(b), is plotted with p on a logarithmic scale the set of curves become a set of parallel lines of slope $-\lambda$, in Fig. 5.15(c).

5.12 Hardening and Softening

At this stage we must return to consider certain special circumstances in which an inward probing vector must be associated with *unstable* yielding of Granta-gravel.

Whenever yielding does occur the specimen will suffer permanent deformation $(\dot{v}, \dot{\epsilon})$ so that after removal of the probe the specimen will have (marginally) changed its specific volume from v_1 to $(v_1 + \delta v) = (v_1 - \dot{v})$ and it will then be in state $(p_s, v_1 - \dot{v}, q_s)$. From the point of view of the observations that can be made by the external agency the specimen will have been distorted into a different rigid specimen of specific volume $(v_1 - \dot{v})$, which in effect is a different material with its own distinct yield curve. It will not be possible to reverse this process to return the specimen to its original state at S.

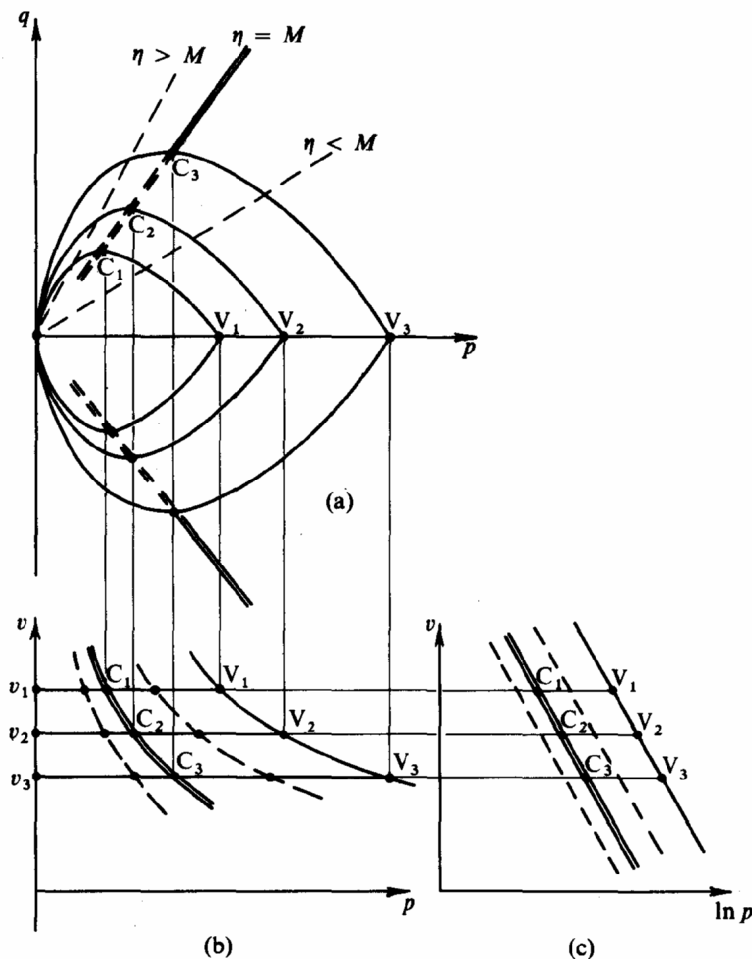


Fig. 5.15 Set of Specimens Yielding at Same Stress Ratio

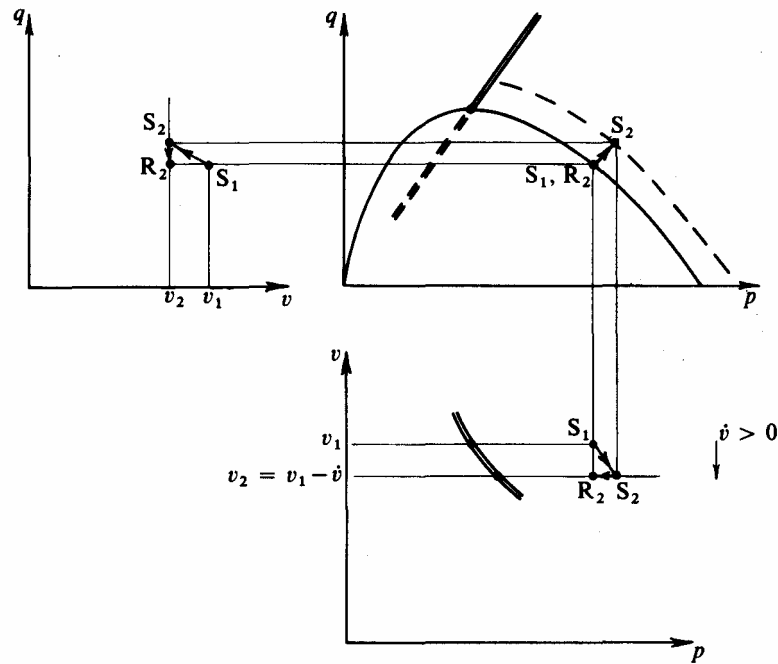


Fig. 5.16 Hardening

From §5.9 it is apparent that the critical curve divides all possible states of a specimen into two distinct categories. Let us first concentrate on specimens which are *weak at yield* for which $0 < q_s < Mp_s$, and show that the application of a small outward probing cycle is consistent with *stable yielding* and permanent deformation ($\dot{v}, \dot{\epsilon} > 0$) to an isotropically hardened state.

From eq. (5.12a) we know that this volumetric strain-increment \dot{v} must be positive, thus δv is negative and the specimen will compact to a smaller total volume $v_2 = (v_1 + \delta v) = (v_1 - \dot{v})$, at which it has a new larger yield curve. On removal of the load-increment to complete the probing cycle as illustrated in Fig. 5.16, the specimen is left in the rigid stressed state ($p_r = p_s, v_2 = v_1 - \dot{v}, q_r = q_s$) which is represented by the point R_2 , *inside* the dotted yield curve that is appropriate to specimens of specific volume v_2 . We could now add a *permanent* load-increment of (\dot{p}, \dot{q}) to our new ‘denser’ specimen at R_2 before bringing it to the verge of yielding again at some point S_2 on the *larger* yield curve. The effect of our probe has been to deform the specimen into one that is slightly stronger or harder, so that our original assumption of stable yielding is valid. This phenomenon is known as *hardening* and will be the consequence of any outward probe that we choose to apply to a specimen with stressed state $0 < q_s < Mp_s$.

In contrast, let us now consider a similar specimen which is in a stressed state F_1 given by (p_f, v_1, q_f) in Fig. 5.17, where it is *strong at yield* with $q_f > Mp_f$. We will now find that yielding has to be associated with application of an inward probe, and this is consistent with *instability*. If the probing causes the specimen to yield and undergo permanent deformation ($\dot{v}, \dot{\epsilon} > 0$) then in this case the volumetric strain-increment \dot{v} must be negative, the sample must expand to a *larger* volume $v_3 = v_1 + \delta v > v_1$, and in this condition at H_3 the new ‘looser’ specimen is just in equilibrium governed by a *smaller* yield curve. Hence the probing cycle had to be directed *inwards* and it will now be impossible to complete the cycle and restore the state to (p_f, q_f) because this state lies outside the dotted yield curve and the specimen can no longer sustain these stresses in

equilibrium. This means that the effect of probing has been to deform the specimen into one that is weaker or softer: we will call this process *softening*.

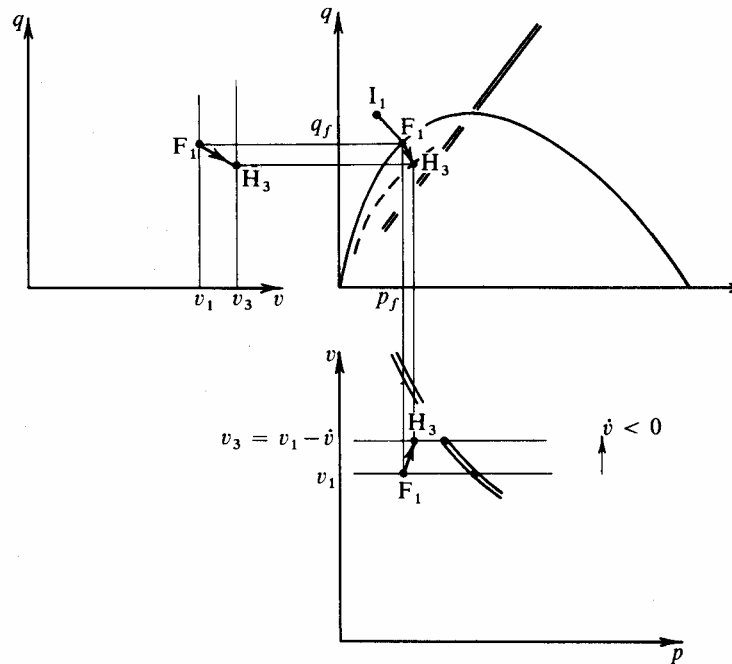


Fig. 5.17 Softening

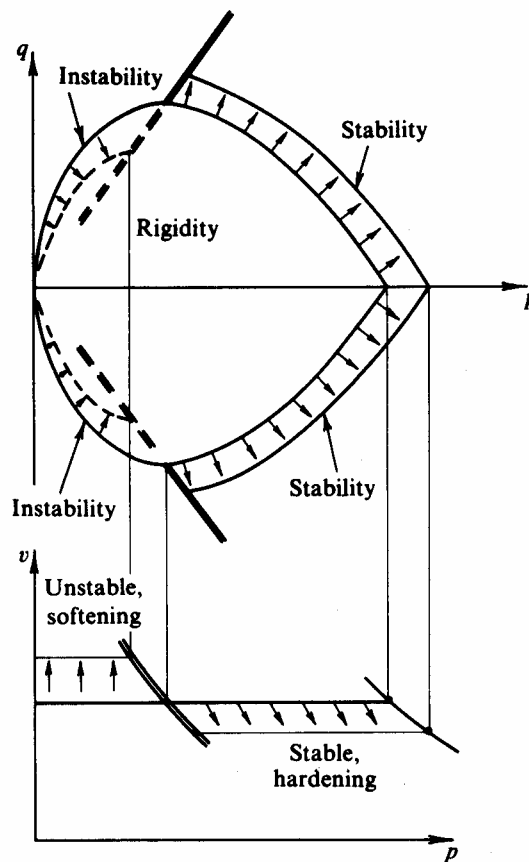


Fig. 5.18 Rigidity, Stability, and Instability

In engineering terms the condition of the specimen at F is what we would recognize as a state of incipient failure, and we would need some buffer to arrest displacements if we were to try to control the specimen and reduce loads during the softening process. Of course if we had tried to apply an outward probe such as F_1I_1 to the original specimen we should have observed catastrophic uncontrollable failure.

The results of probing both categories of specimen are summarized in Fig. 5.18.

5.13 Comparison with Real Granular Materials

At this stage we need to take stock of the development of Granta-gravel as an ideal artificial material and see whether it has developed into a useful model and whether its behaviour bears meaningful and worthwhile resemblance to that of real granular materials. We have established certain important features of its behaviour and seen what a dominant role the line of critical states plays in dividing the states of the material into those in which it will display continuous stable yielding and ‘harden’ from those in which it will ‘fail’ in unstable yielding and ‘soften’.

In our test system we are considering the application of small fixed increments of load and imitating a stress controlled test. In reality most modern laboratory testing is conducted in a strain-controlled manner, but for the results to be valid the rate of strain must be sufficiently slow that pore-pressure gradients are negligible at all times. This will be equivalent to applying a continuous sequence of infinitesimal load-increments of different intensity so that the rate of strain is constant, i.e., $\dot{\epsilon} \propto \dot{t}$. It will consequently be legitimate for us to predict what the results of strain-controlled tests on Granta-gravel would be, from our ‘stress-controlled theory’.

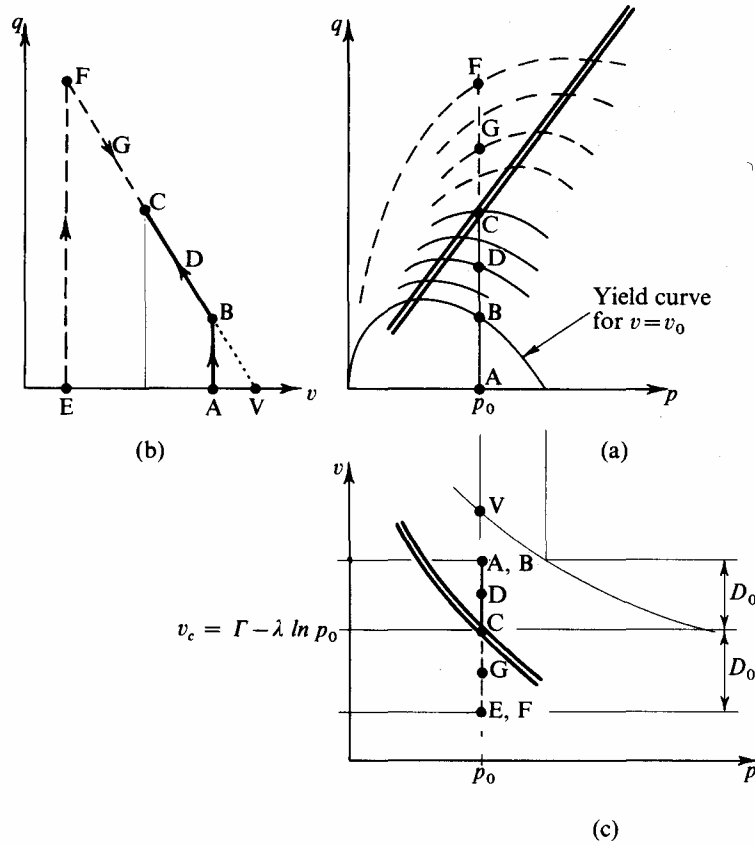
For simplicity, let us consider a compression test on a specimen of initial state $(p_0, v_0, q=0)$ in which at all times the effective spherical pressure p is held constant at p_0 , so that $\dot{p} = 0$. The state of the specimen throughout the test must lie in the $p = p_0$ plane, which intersects the positive half of the state boundary surface in the straight line

$$p = p_0 \quad \frac{\lambda q}{Mp_0} = (\lambda + \Gamma - \lambda \ln p_0) - v \quad (5.32)$$

obtained directly from eq. (5.30), and shown in Fig. 5.19 in the three projected views of the stable-state boundary surface containing all the points A, B, C, D, E, F, G, and V.

If the initial condition is such that $v_0 > (\Gamma - \lambda \ln p_0)$ the specimen will start at state A, in a condition looser or wetter than critical. As the axial-deviator stress is increased the specimen will remain rigid until it yields at B (when it reaches the yield curve corresponding to $v = v_0$) and then continue to yield in a stable *hardening* manner up BDC until it eventually reaches the critical state at C after infinite strain.

Conversely, a specimen with $v_0 < (\Gamma - \lambda \ln p_0)$ will start at state E in a condition denser or drier than critical. The specimen remains rigid until it reaches state F and thereafter exhibits unstable *softening* down FGC until it reaches the critical state at C, after infinite strain.

Fig. 5.19 Constant- p Test Paths

For convenience, let Z always be used to denote the point in (p, v, q) space representing the current state of the specimen at the particular stage of the test under consideration. As the test progresses the passage of Z on the state boundary surface either from B up towards C, or from F down towards C will be exactly specified by the set of three equations:

$$\left. \begin{aligned} \frac{p\dot{v}}{v} + q\dot{\varepsilon} &= Mp\dot{\varepsilon} & (\dot{\varepsilon} > 0) \text{ (5.19 bis)} \\ q &= \frac{Mp}{\lambda}(\lambda + \Gamma - v - \lambda \ln p) & (q > 0) \text{ (5.30 bis)} \\ p &= \text{constant} = p_0. \end{aligned} \right\} \quad (5.33)$$

The first two equations govern the behaviour of all specimens and the third is the restriction on the test path imposed by our choice of test conditions for this specimen. We will find it convenient in a constant- p test to relate the initial state of the specimen to its ultimate critical state by the total change in volume represented by the distance AC (or EC) in Fig. 5.19(c) and define

$$D_0 = v_0 - v_c = v_0 - \Gamma + \lambda \ln p_0. \quad (5.34)$$

The conventional way of presenting the test data would be in plots of axial-deviator stress q against cumulative shear strain ε and total volumetric strain $\Delta v/v_0$ against ε , and this can be achieved by manipulating equations (5.33) as follows. From the last two equations and (5.34) we have

$$\lambda q = Mp_0(v_0 - v + \lambda - D_0)$$

and substituting in the first equation

$$\frac{p_0 \dot{v}}{v} = (Mp_0 - q)\dot{\varepsilon} = \frac{Mp_0 \dot{\varepsilon}}{\lambda} (v - v_0 + D_0).$$

Remembering that $\dot{\varepsilon} = +\delta\varepsilon$ whereas $\dot{v} = -\delta v$ this becomes

$$\frac{M}{\lambda} \frac{d\varepsilon}{dv} = \frac{-1}{v(v - v_0 + D_0)} = \frac{1}{(v_0 - D_0)} \left\{ \frac{1}{v} - \frac{1}{(v - v_0 + D_0)} \right\}. \quad (5.35)$$

Integrating $\frac{M}{\lambda} \varepsilon = \frac{1}{v_0 - D_0} \ln \left\{ \frac{v}{v - v_0 + D_0} \right\} + \text{constant}$

and if ε is measured from the beginning of the test

$$M\varepsilon = \frac{\lambda}{v_0 - D_0} \ln \left\{ \frac{D_0 v}{v_0 (v - v_0 + D_0)} \right\}$$

i.e.,

$$\exp \left\{ -\frac{M(v_0 - D_0)}{\lambda} \varepsilon \right\} = \frac{v_0 (v - v_0 + D_0)}{D_0 v} = \frac{v_0 (\Delta v + D_0)}{D_0 (\Delta v + v_0)} \quad (5.36)$$

which is the desired relationship between $\Delta v/v_0$ and ε .

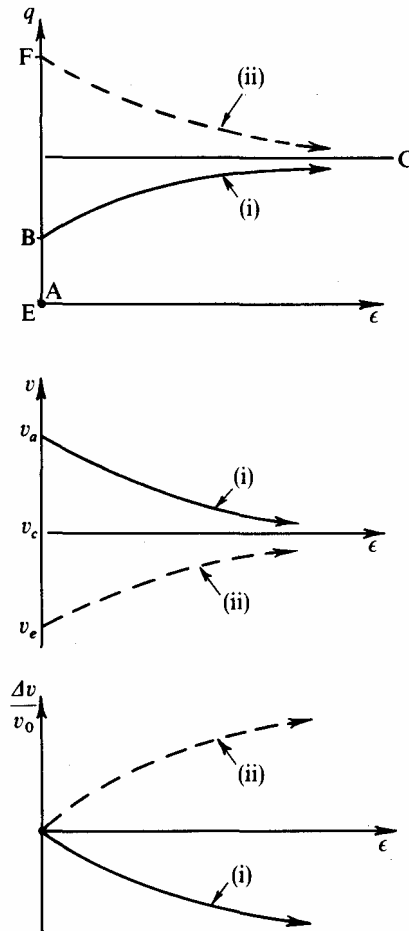


Fig. 5.20 Constant-p Test Results

Similarly we can obtain q as a function of ϵ

$$\exp\left\{-\frac{M(v_0 - D_0)}{\lambda}\epsilon\right\} = \frac{v_0\lambda(Mp_0 - q)}{D_0[Mp_0(v_0 - D_0 + \lambda) - \lambda q]} \quad (5.37)$$

These relationships for (i) a specimen looser than critical and (ii) a specimen denser than critical are plotted in Fig. 5.20 and demonstrate that we have been able to describe a complete strain-controlled constant- p axial-compression test on a specimen of Granta-gravel.

In a similar manner we could describe a conventional drained test in which the cell pressure σ_r is kept constant and the axial load varies as the plunger is displaced at a constant rate. In §5.5 we saw that throughout such a test $\dot{p} = \frac{1}{3}\dot{q}$, so that the state of the specimen, Z , would be confined at all times to the plane $p = p_0 + \frac{1}{3}q$. Hence the section of this 'drained' plane with the state boundary surface is very similar to the constant- p test of Fig. 5.19 except that the plane has been rotated about its intersection with the $q = 0$ plane to make an angle of $\tan^{-1} 3$ with it.

The differential equation corresponding to eq. (5.35) is not directly integrable, but gives rise to curves of the same form as those of Fig. 5.20.

An attempt to compare these with actual test results on cohesion-less granular materials is not very fruitful. Such specimens are rarely in a condition looser than critical; when they are, it is usually because they are subject to high confining pressures outside the normal range of standard laboratory axial-test equipment. Among the limited published data is a series of drained tests on sand and silt by Hirschfeld and Poulos¹², and the 'loosest' test quoted on the sand is reproduced in Fig. 5.21 showing a marked resemblance to the behaviour of constant- p tests for Granta-gravel.

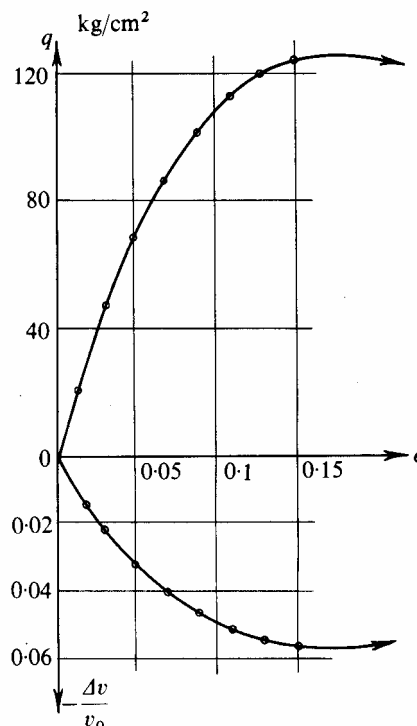


Fig. 5.21 Drained Axial Test on Sand (After Hirschfeld & Poulos)

For the case of specimens denser than critical, Granta-gravel is rigid until peak deviator stress is reached, and we shall not expect very satisfactory correlation with experimental results for strains after peak on account of the instability of the test system

and the non-uniformity of distortion that are to be expected in real specimens. This topic will be discussed further in chapter 8.

However, it is valuable to compare the predictions for peak conditions such as at state F of Fig. 5.19 and this will be done in the next section.

5.14 Taylor's Results on Ottawa Sand

In chapter 14 of his book¹³ *Fundamentals of Soil Mechanics* Taylor discusses in detail the shearing characteristics of sands and uses the word 'interlocking' to describe the effect of dilatancy. He presents results of direct shear tests in which the specimen is essentially experiencing the conditions of Fig. 5.22(a); the direct shear apparatus is described in Taylor's book, and the main features can be seen in the Krey shear apparatus of Fig. 8.2. In these tests the vertical effective stress σ' was held constant, and the specimens all apparently denser than critical were tested in a fully air-dried condition, i.e., there was no water in the pore space. (It is well established that sand specimens will exhibit similar behaviour to that illustrated in Fig. 5.22(b) with voids either completely empty or completely full of water, provided that the drainage conditions are the same.)

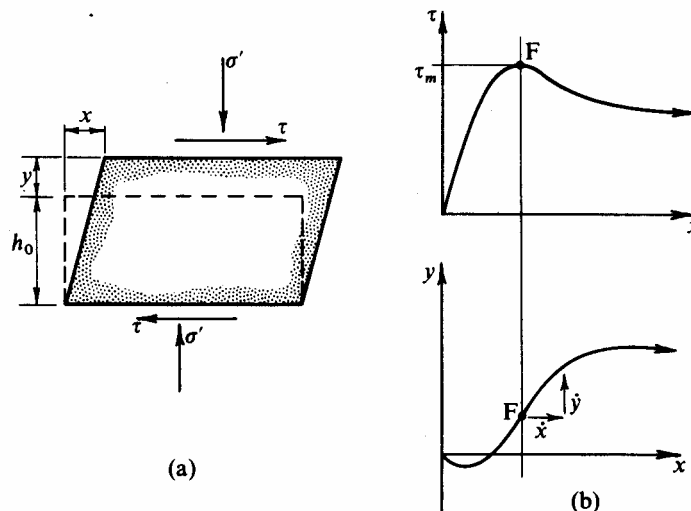


Fig. 5.22 Results of Direct Shear Tests on Sand

On page 346 of his book, Taylor calculates the loading power being supplied to the specimen making due allowance for the external work done by the interlocking or dilatation. In effect, he calculates for the peak stress point F the expression

$$\tau A \dot{x} - \sigma' A \dot{y} = \mu \sigma' A \dot{x} \quad (5.38)$$

(total loading power = frictional work)

which has been written in our terminology, and where A is the cross-sectional area of the specimen. This is directly analogous to eq. (5.19),

$$q \dot{\epsilon} + \frac{p \dot{v}}{v} = Mp |\dot{\epsilon}|$$

which relates true stress invariants p and q , and which expresses the loading power per unit volume of specimen. The parameters are directly comparable: q with τ , p with σ' , $\dot{\epsilon}$ with \dot{x} , and \dot{v}/v with $-\dot{y}$ (opposite sign convention); and so we can associate Taylor's approach with the Granta-gravel model.

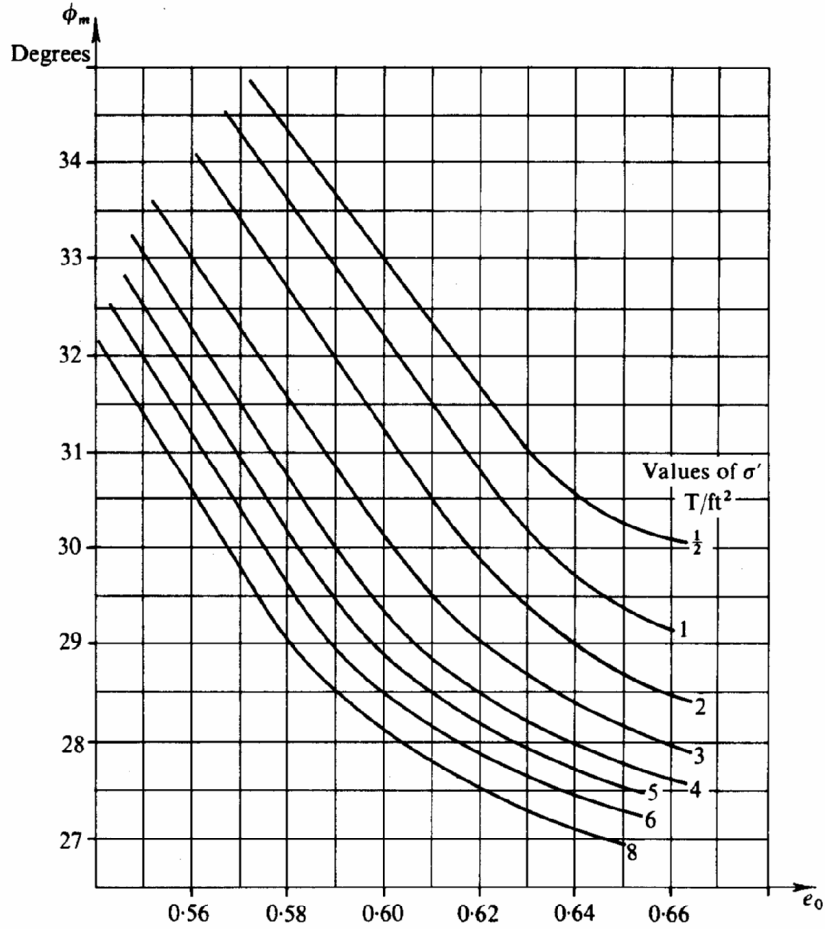


Fig. 5.23 Friction Angle Data from Direct Shear Tests (Ottawa Standard Sand) (After Taylor)

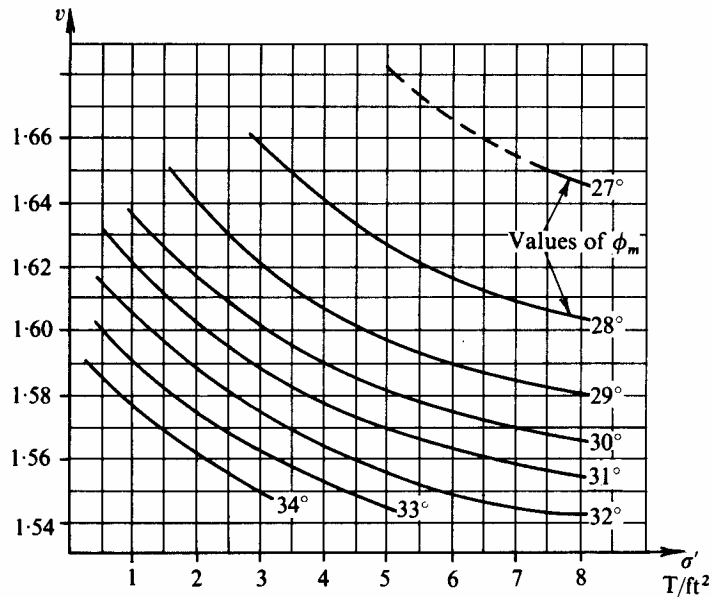


Fig. 5.24 Friction Angle Data from Direct Shear Tests replotted from Fig. 5.23

The comparison can be taken a stage further than this. In his Fig. 14.10, reproduced here as Fig. 5.23, Taylor shows the variation of peak friction angle ϕ_m (where $\tan \phi_m = \tau_m/\sigma'$) with initial voids ratio e_0 for different values of fixed normal stress σ' . These results have

been directly replotted in Fig. 5.24 as curves of constant ϕ_m (or peak stress ratio τ_m/σ'_r) for differing values of $v = (1 + e)$ and σ'_r .

There is a striking similarity with Fig. 5.15(b) where each curve is associated with a set of Granta-gravel specimens that have the same value of q/p at yield. Taylor suggests an ultimate value of ϕ for his direct shear tests of 26.7° which can be taken to correspond to the critical state condition, so that all the curves in Fig. 5.24 are on the dense side of the critical curve.

5.15 Undrained Tests

Having examined the behaviour of Granta-gravel in constant- p and conventional drained tests, we now consider what happens if we attempt to conduct an undrained test on a specimen. In doing so we shall expose a deficiency in the model formed by this artificial material.

It is important to appreciate that in our test system of Fig. 5.4, although there are three separate platforms to each of which we can apply a load-increment, \dot{X}_i , we only have two degrees of freedom regarding our choice of probe (\dot{p}, \dot{q}) experienced by the specimen. This is really a consequence of the principle of effective stress, in that the behaviour of the specimen in our test system is controlled by two effective stress parameters which can be either the pair (σ'_l, σ'_r) or (p, q) . The effects of the loads on the cell-pressure and pore-pressure platforms are *not* independent; they combine to control the effective radial stress σ'_r experienced by the specimen.

Throughout a conventional *drained* test we choose to have zero load-increments on the pore-pressure and cell-pressure platforms ($\dot{X}_1 = \dot{X}_2 \equiv 0$) and to deform the specimen by means of varying the axial load-increment \dot{X}_3 , and allowing it to change its volume.

In contrast, in a conventional *undrained* test we choose to have zero load-increment \dot{X}_2 on the cell-pressure platform only, and to deform the specimen by means of varying the axial load-increment \dot{X}_3 . However, we can only keep the specimen at constant volume by applying a simultaneous load-increment \dot{X}_1 of a specific magnitude which is *dictated* by the response of the specimen. Hence for any choice of made by the external agency, the specimen will require an associated \dot{X}_1 if its volume is to be kept constant.

Let our specimen of Granta-gravel be in an initial state $(p_1, v_0, q = 0)$ represented by I in Fig. 5.25. As we start to increase the axial load by a series of small increments \dot{X}_3 , the specimen remains rigid and has no tendency to change volume so that the associated \dot{X}_1 are all zero. Under these conditions there is no change in pore-pressure and $\dot{p} = \frac{1}{3}\dot{q}$ so that the point Z representing the state of the sample starts to move up the line IJ of slope 3.

This process will continue until Z reaches the yield curve, appropriate to $v = v_0$, at point K. At this stage of the test in order that the specimen should remain at constant volume, Z cannot go outside the yield curve (otherwise it would result in permanent \dot{v} and \dot{e}); thus as q further increases the only possibility is for Z to progress *along* the yield curve in a series of steps of *neutral change*. Once past the point K, the shape of the yield curve will dictate the magnitude of \dot{X}_1 that is required for each successive \dot{X}_3 . At a point such as L the required $\sum \dot{X}_1$ will be represented by the distance $LM = p_0 + \frac{1}{3}q - p$, so that this offset indicates the total increase of pore-pressure experienced by the specimen.

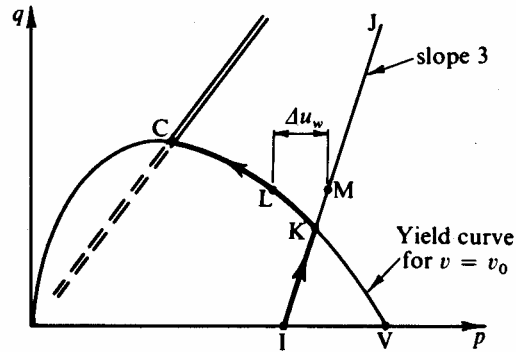


Fig. 5.25 Undrained Test Path for Loose Specimen of Granta-gravel

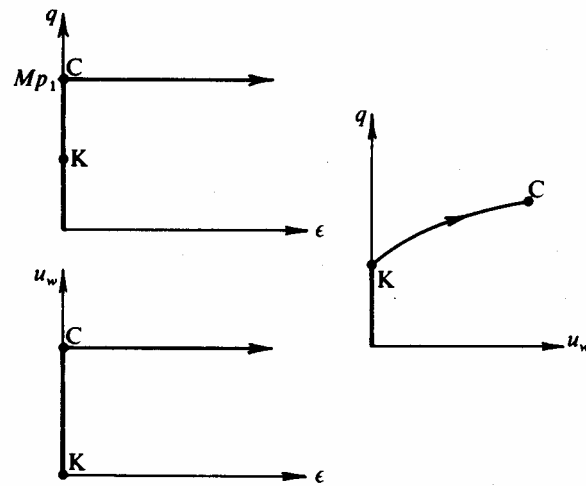


Fig. 5.26 Undrained Test Results for Loose Specimen of Granta-gravel

Eventually the specimen reaches the critical state at C when it will deform at constant volume with indeterminate distortion ϵ . The conventional plots of deviator stress and pore-pressure against shear strain ϵ will be as shown in Fig. 5.26, indicating a rigid/perfectly plastic response.

As mentioned in §5.13, when comparing the behaviour in drained tests of Granta-gravel with that of real cohesionless materials, it is rare to find published data of tests on specimens in a condition looser than critical. However, some undrained tests on Ham River sand in this condition have been reported by Bishop¹⁴; and the results of one of these tests have been reproduced in Fig. 5.27. (This test is No. 9 on a specimen of porosity 44.9 per cent, i.e., $\nu = 1.815$; it should be noted that for an *undrained* test $\dot{\nu}/\nu = \dot{\epsilon}_1 + 2\dot{\epsilon}_3 \equiv 0$ so that $\dot{\epsilon} = \frac{2}{3}(\dot{\epsilon}_1 - \dot{\epsilon}_3) = \dot{\epsilon}_1 = \text{axial strain.}$)

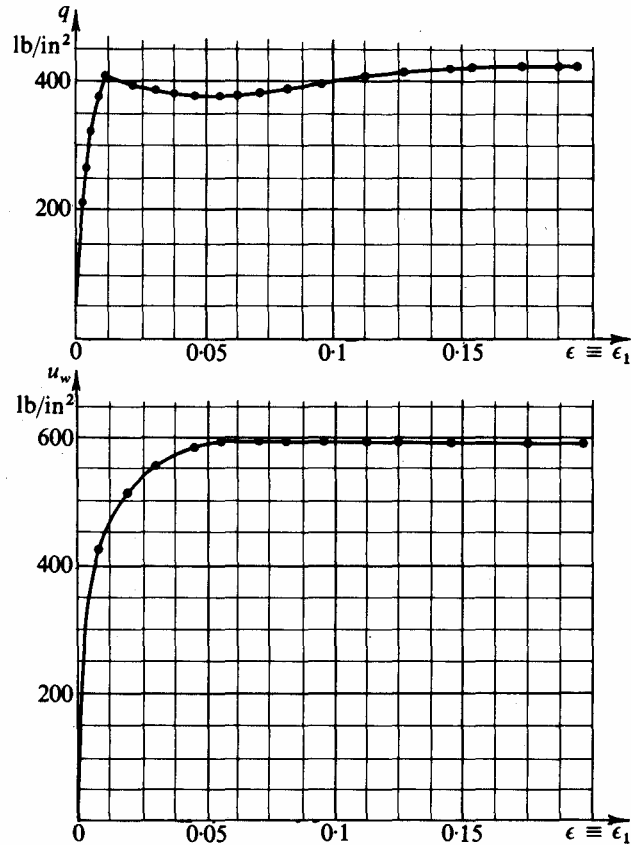


Fig. 5.27 Undrained Test Results on very Loose Specimen of Ham River Sand (After Bishop)

The results show a close similarity to that of Fig. 5.26. In particular it is significant that axial-deviator stress reaches a peak at a very small axial strain of only about 1 per cent, whereas in a drained test on a similar specimen at least 15–20 per cent axial strain is required to reach peak. We can compare Bishop's test results of Fig. 5.27 with Hirschfeld and Poulos¹² test results of Fig. 5.21. These figures may be further compared with Fig. 5.26 and 5.20 which predict extreme values for Granta-gravel which are respectively zero strain and infinite strain to reach peak in undrained and drained tests.

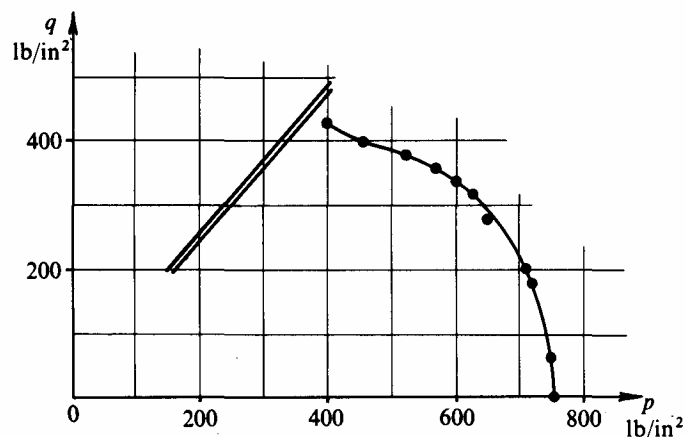


Fig. 5.28 Undrained Test Path for very 'Loose' Specimen of Ham River Sand

Although the Granta-gravel model is seen to be deficient in not allowing us to estimate any values of strains during an undrained test, we can get information about the stresses. The results of Fig. 5.27 have been re-plotted in Fig. 5.28 and need to be compared

with the path IKLC of Fig. 5.25. An accurate assessment of how close the actual path in Fig. 5.28 is to the shape of the yield curve is presented in Fig. 5.29 where q/p has been plotted against $\ln(p/p_u)$, and the yield curve becomes the straight line

$$\frac{q}{p} = M[1 - \ln(p/p_u)] \tag{5.27 bis}$$

The points obtained for the latter part of the test lie very close to a straight line and indicate a value for M of the order of 1.2, but this value will be sensitive to the value of p_u chosen to represent the critical state.

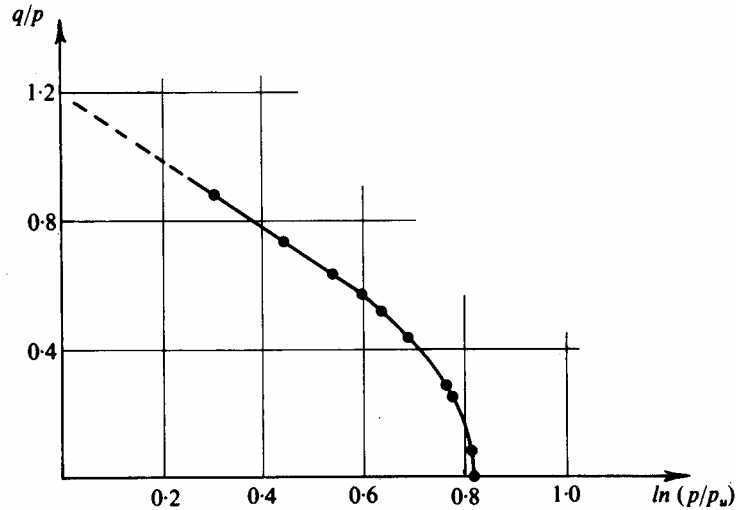


Fig. 5.29 Undrained Test Path Replotted from Fig. 5.28

Consideration of undrained tests on specimens denser than critical leads to an anomaly. If the specimen is in an initial state at a point such as I in Fig. 5.30 we should expect the test path to progress up the line IJ until the yield curve is reached at K and then move round the yield curve until the critical state is reached at C. However, experience suggests that the test path for real cohesionless materials turns off the line IJ at N and progresses up the straight line NC which is collinear with the origin.

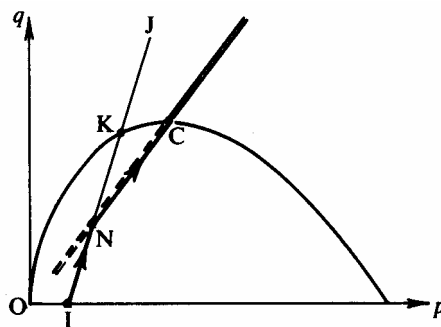


Fig. 5.30 Undrained Test Path for Dense Specimen of Granta-gravel

At the point N, and anywhere on NC, the stressed state of the specimen $q = Mp$ is such that in the initial specification of Granta-gravel, we have the curious situation in which the power eq. (5.19) (for $\dot{\epsilon} \geq 0$)

$$\frac{p\dot{v}}{v} + q\dot{\epsilon} = Mp\dot{\epsilon}$$

is satisfied for *all* values of $\dot{\epsilon}$, since $\dot{v} \equiv 0$. Moreover, the stability criterion is also satisfied so long as $\dot{q} > 0$, which will be the case. Hence it is quite possible for the test path to take

a short cut by moving up the line NC while still fulfilling the conditions imposed on the test system by the external agency. This, together with the occurrence of instability when specimens yield with $q > Mp$ (as shown in Fig. 5.18), lead us to regard the plane $q = Mp$ as forming a boundary to the domain of stable states. Our Fig. 5.14 therefore must be modified: the plane containing the line $C_1C_2C_3C_4$ and the axis of v will become a boundary of the stable states instead of the curved surface shown in Fig. 5.14. This modification has the fortunate consequence of eliminating any states in which the material experiences a *negative* principal stress, and hence we need not concern ourselves with the possibility of tension-cracking.

5.16 Summary

In this chapter we have investigated the behaviour of the artificial material Granta-gravel and seen that in many respects this does resemble the general pattern of behaviour of real cohesionless granular materials. The model was seen to be deficient (5. 15) regarding undrained tests in that no distortion whatsoever occurs until the stresses have built up to bring the specimen into the critical state appropriate to its particular volume. This difficulty can be overcome by introducing a more sophisticated model, Cam-clay, in the next chapter, which is not rigid/perfectly plastic in its response to a probe.

In particular, the specification of Granta-gravel can be summarized as follows:

(a) No recoverable strains

$$\dot{v}^r \equiv \dot{\varepsilon}^r \equiv 0$$

(b) Loading power all dissipated

$$\frac{p\dot{v}}{v} + q\dot{\varepsilon} = Mp|\dot{\varepsilon}| \quad (5.19 \text{ bis})$$

(c) Equations of critical states

$$|q| = Mp \quad (5.22 \text{ bis})$$

$$v = \Gamma - \lambda \ln p \quad (5.23 \text{ bis})$$

References to Chapter 5

- ¹ Prager, W. and Drucker, D. C. Soil Mechanics and Plastic Analysis or Limit Design', *Q. Appl. Mathematics*, **10: 2**, 157 – 165, 1952.
- ² Drucker, D. C., Gibson, R. E. and Henkel, D. J. 'Soil Mechanics and Work hardening Theories of Plasticity', *A.S.C.E.*, **122**, 338 – 346, 1957.
- ³ Drucker, D. C. 'A Definition of Stable Inelastic Material', *Trans. A.S.M.E. Journal of Appl. Mechanics*, **26: 1**, 101 – 106, 1959.
- ⁴ Roscoe, K. H., Schofield, A. N. and Thurairajah, A. Correspondence on 'Yielding of clays in states wetter than critical', *Géotechnique*, **15**, 127 – 130, 1965.
- ⁵ Drucker, D. C. 'On the Postulate of Stability of Material in the Mechanics of Continua', *Journal de M'canique*, Vol. **3**, 235 – 249, 1964.
- ⁶ Schofield, A. N. *The Development of Lateral Force during the Displacement of Sand by the Vertical Face of a Rotating Mode/Foundation*, Ph.D. Thesis, Cambridge University, 1959. pp. 114 – 141.
- ⁷ Hill, R. *Mathematical Theory of Plasticity*, footnote to p. 38, Oxford, 1950.
- ⁸ Wroth, C. P. *Shear Behaviour of Soils*, Ph.D. Thesis, Cambridge University, 1958.
- ⁹ Poorooshasb, H. B. *The Properties of Soils and Other Granular Media in Simple Shear*, Ph.D. Thesis, Cambridge University. 1961.

- ¹⁰ Thurairajah, A. *Some Shear Properties of Kaolin and of Sand*. Ph.D. Thesis, Cambridge University. 1961.
- ¹¹ Bassett, R. H. Private communication prior to submission of Thesis, Cambridge University, 1967.
- ¹² Hirschfeld, R. C. and Poulos, S. J. 'High-pressure Triaxial Tests on a Compacted Sand and an Undisturbed Silt', *A.S.T.M. Laboratory Shear Testing of Soils Technical Publication No. 361*, 329 – 339, 1963.
- ¹³ Taylor, D. W. *Fundamentals of Soil Mechanics*, Wiley, 1948.
- ¹⁴ Bishop, A. W. 'Triaxial Tests on Soil at Elevated Cell Pressures', *Proc. 6th Int. Conf. Soil Mech. & Found. Eng.*, Vol. 1, pp. 170 – 174, 1965.